Supporting Information

Dual-Responsive BN-Embedded Phenacenes Featuring Mechanochromic Luminescence and Ratiometric Sensing of Fluoride Ion

Yi Han, Wei Yuan, Hongyan Wang, Mengwei Li, Wenqin Zhang and Yulan Chen*

Tianjin Key Laboratory of Molecular Optoelectronic Science, Department of Chemistry,

Tianjin University, Tianjin, 300354, P. R. China

E-mail: yulan.chen@tju.edu.cn.

Experimental Section

Materials: Unless noted otherwise, all chemicals were purchased from Aldrich or Acros and used without further purification. 3,6-Di(thiophen-2-yl)benzene-1,2-diamine,[1] 4,9-dibromo-[1,2,5]thiadiazolo[3,4-*g*]quinoxaline (**1**),[2] 2-(tri-n-butylstannyl)thiophene[3] and 2-(tri-*n*-butylstannyl)benzothiophene[4] were prepared according to literatures. Dichloromethane (CH_2Cl_2) was distilled over CaH_2. Tetrahydrofuran (THF) was distilled over sodium and benzophenone. All reactions were performed under an atmosphere of nitrogen and monitored by TLC with silica gel 60 F254 (Merck, 0.2 mm). Column chromatography was carried out on silica gel (200-300 mesh).

Characterization: ^1H and ^{13}C NMR spectra were recorded on a Bruker AV400 spectrometer in $CDCl_3$. High resolution mass spectra (ESI-TOF) were recorded from Perkin-Elmer TURBOMASS instrument. UV-vis absorption spectra were obtained on a PerkinElmer Lambda 750 UV/VIS/NIR spectrometer. Photoluminescent (PL) spectra were recorded on a Hitachi F-7000 spectrometer. Thermogravimetric analyses (TGA) were carried out using a TA Instruments Q-50 with a heating rate of 10 °C/min. Differential scanning calorimetry (DSC) measurements were conducted using the TA Instruments Q-20 with a scan rate of 10 °C/min. The powder XRD patterns were obtained with a Rigaku SmartLab (9 kW) X-ray diffractometer. The single crystal X-ray diffraction was recorded on a Rigaku SCX-mini diffractometer with graphite monochromatic Mo-Kα radiation (λ = 0.7173 Å) by ω scan mode. The absolute fluorescence quantum yields were measured by using an absolute PL quantum yield spectrometer (Edinburg FLS-920 fluorescence spectrometer) with a calibrated integrating sphere and fluorescence lifetime measurements were recorded on the same spectrometer using time-correlated single photon counting (TCSPC). Cyclic voltammetric experiments were carried out using a CHI 660E electrochemical workstation (CHInstruments, ChenHua, Shanghai, China). All voltammograms were acquired at room temperature. A standard three electrode electrochemical cell arrangement was employed using a glassy

carbon (GC) as working electrode, a Pt wire as counter electrode, and a standard calomel electrode (SCE) as reference electrode in 0.1 M tetrabutylammonium hexafluorophosphate (*n*-Bu_4NPF_6) as the supporting electrolyte at the scan rate of 100 mV/s. The potentials are reported *vs* the Fc^+/Fc redox couple as a standard. Density functional theory (DFT) calculations were performed in Gaussian 09 software at the B3LYP functional with the 6-31G* basis set level. The ^{13}C cross-polarization magic angle spinning (CP/MAS) spectra were recorded with a 4 mm double-resonance MAS probe and at a MAS rate of 10.0 kHz with a contact time of 2 ms (ramp 100) and a pulse delay of 3 s.

Synthesis:

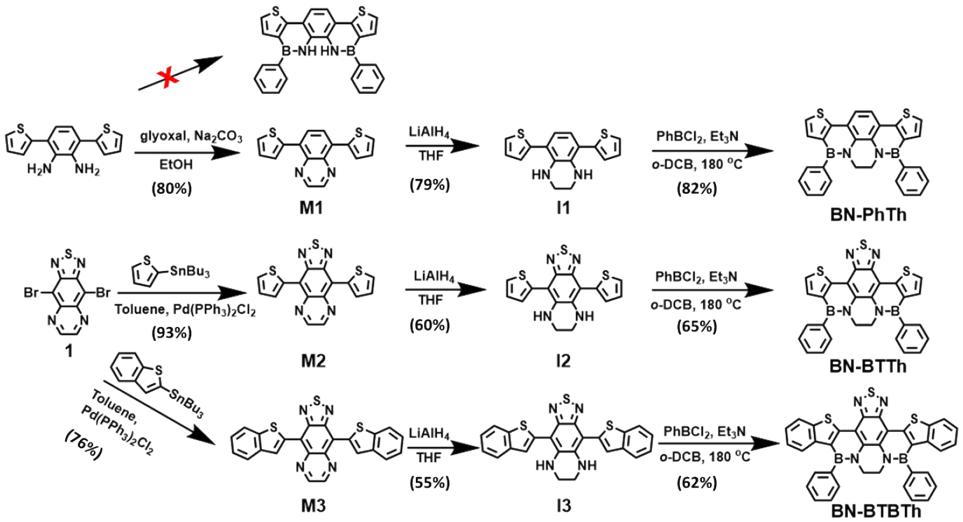

5,8-Di(thiophen-2-yl)quinoxaline (M1). To a solution of 3,6-di(thiophen-2-yl)benzene-1,2-diamine (1.00 g, 3.67 mmol) in ethanol (50 mL) under argon was added glyoxal (40% in water) (1.16 mL, 7.92 mmol) and Na_2CO_3 (3.89 g, 36.70 mmol). The reaction mixture was refluxed for 2 h and the solution turned yellow. Then, water was added (50 mL) and the product was extracted by 3 x 50 mL of dichloromethane. The organic phase was dried over $MgSO_4$ and the solvent was evaporated. The product was purified by chromatography on silica gel to give product **M1** as a yellow powder (1.06 g, 80%). m.p., 137.2–138.5 °C. ^1H NMR (400 MHz, $CDCl_3$): δ 8.94 (s, 2H), 8.08 (s, 2H), 7.79 (dd, J = 3.7, 1.0 Hz, 2H), 7.50 (dd, J = 5.1, 1.0 Hz, 2H), 7.18 (dd, J = 5.1, 3.7 Hz, 2H). ^{13}C NMR (100 MHz, $CDCl_3$): δ 143.6,

139.9, 138.5, 132.1, 128.5, 127.9, 127.2, 126.9. HRMS (ESI-TOF) m/z: $[M + H]^+$ Calcd for $C_{16}H_{11}N_2S_2$ 295.0364; Found 295.0364.

General Procedure for the Synthesis of M2 and M3. A mixture of the precursor **1**, tributyltin derivatives of thiophene or benzothiophene and THF/toluene (v/v, 1:1) was carefully degassed before and after $Pd(PPh_3)_2Cl_2$ was added. The mixture was heated to reflux and stirred under nitrogen overnight. CH_2Cl_2 and brine was added, and the organic layer was separated and dried over anhydrous Na_2SO_4. After the removal of the solvent, the residue was purified by chromatography on a silica gel column to afford the desired product (**M2**, **M3**). Owing to their poor solubilities, the ^1H and ^{13}C NMR of **M2** and **M3** cannot be measured in $CDCl_3$ solution.

4,9-Di(thiophen-2-yl)-[1,2,5]thiadiazolo[3,4-*g*]quinoxaline (M2). Compound **1** (1.00 g, 2.89 mmol), tributyl(thiophen-2-yl)stannane (2.70 g, 7.23 mmol), $Pd(PPh_3)_2Cl_2$ (20.28 mg, 0.29 mmol), THF (50 mL) and toluene (50 mL) were used, and CH_2Cl_2/THF (v/v, 10:1) was used as the eluent to afford **M2** as a blue solid (950 mg, 93%). m.p., 143.5–144.7 °C. HRMS (ESI-TOF) m/z: $[M + H]^+$ Calcd for $C_{16}H_9N_4S_3$ 352.9989; Found 352.9989.

4,9-Bis(benzo[*b*]thiophen-2-yl)-[1,2,5]thiadiazolo[3,4-*g*]quinoxaline (M3). Compound **1** (1.00 g, 2.89 mmol), benzo[*b*]thiophen-2-yltributylstannane (3.06 g, 7.23 mmol), $Pd(PPh_3)_2Cl_2$ (20.28 mg, 0.29 mmol), THF (50 mL) and toluene (50 mL) were used, and CH_2Cl_2/THF (v/v, 10:1) was used as the eluent to afford **M2** as a blue solid (1.00 g, 76%). m.p., 151.8–153.2 °C. HRMS (ESI-TOF) m/z: $[M + H]^+$ Calcd for $C_{24}H_{13}N_4S_3$ 453.0302; Found 453.0302.

General Procedure for the Synthesis of I1, I2 and I3. To a solution of precursor **M1**-**M3** in THF under argon was added $LiAlH_4$. The reaction mixture was stirred for 1 h at the room temperature. Then water was added and the product was extracted by ethyl acetate. The

organic phase was dried over $MgSO_4$ and the solvent was evaporated. Quick filtration through a silica gel plug gave intermediate **I1**-**I3**.

5,8-Di(thiophen-2-yl)-1,2,3,4-tetrahydroquinoxaline (I1). M1 (0.50 g, 1.70 mmol), THF (15 mL), $LiAlH_4$ (1.29 g, 34.0 mmol) were used. The reaction mixture was stirred for 1 h and then the solution turned colorless. CH_2Cl_2/*n*-hexane (v/v, 1:1) was used as the eluent to afford **I1** as a white solid (0.40 g, 79%). m.p., 129.5–131.2 °C. ^{1}H NMR (400 MHz, $CDCl_3$): δ 7.35 (d, J = 5.1 Hz, 2H), 7.20 (d, J = 3.5 Hz, 2H), 7.12 (dd, J = 5.1, 3.5 Hz, 2H), 6.72 (s, 2H), 4.47 (s, 2H), 3.43 (s, 4H). ^{13}C NMR (100 MHz, $CDCl_3$): δ 141.2, 131.4, 127.7, 126.1, 125.5, 120.1, 119.0, 41.0. HRMS (ESI-TOF) m/z: $[M + H]^+$ Calcd for $C_{16}H_{15}N_2S_2$ 299.0677; Found 299.0677.

4,9-Di(thiophen-2-yl)-5,6,7,8-tetrahydro-[1,2,5]thiadiazolo[3,4-*g*]quinoxaline (I2). M2 (0.50 g, 1.40 mmol), THF (15 mL), $LiAlH_4$ (1.06 g, 28.0 mmol) were used. The reaction mixture was stirred for 1 h and then the solution turned orange. CH_2Cl_2 was used as the eluent to afford **I2** as a yellow solid (0.30 g, 60%). m.p., 142.2–143.9 °C .^{1}H NMR (400 MHz, $CDCl_3$): δ 7.52 (dd, J = 5.1, 0.7 Hz, 2H), 7.32-7.28 (dd, J = 3.5, 0.7 Hz, 2H), 7.22 (dd, J = 5.1, 3.5 Hz, 2H), 5.24 (s, 2H), 3.45 (s, 4H).^{13}C NMR (100 MHz, $CDCl_3$): δ 150.7, 137.8, 135.3, 128.5, 127.6, 127.1, 103.1, 40.2. HRMS (ESI-TOF) m/z: $[M + H]^+$ Calcd for $C_{16}H_{13}N_4S_3$ 357.0302; Found 357.0302.

4,9-Bis(benzo[*b*]thiophen-2-yl)-5,6,7,8-tetrahydro-[1,2,5]thiadiazolo[3,4-*g*]quinoxaline (I3). M3 (0.50 g, 1.10 mmol), THF (15 mL), $LiAlH_4$ (0.85 g, 22.0 mmol) were used. The reaction mixture was stirred for 1 h and then the solution turned orange. CH_2Cl_2 was used as the eluent to afford **I3** as a yellow solid (0.29 g, 55 %). m.p., 147.5–149.1 °C. ^{1}H NMR (400 MHz, $CDCl_3$): δ 7.91 (d, J = 7.3 Hz, 2H), 7.86 (d, J = 6.92 Hz, 2H), 7.57 (s, 2H), 7.40 (m, 4H), 5.42 (s, 2H), 3.52 (s, 4H). ^{13}C NMR (100 MHz, $CDCl_3$): δ 150.5, 141.0, 140.2, 138.0, 136.0,

125.8, 124.8, 124.6, 124.0, 122.5, 103.5, 40.3. HRMS (ESI-TOF) m/z: $[M + H]^+$ Calcd for $C_{24}H_{17}N_4S_3$ 457.0615; Found 457.0615.

General Procedure for the Synthesis of BN-PhTh, BN-BTTh and BN-BTBTh. Dichlorophenylborane was added to a solution of **I1**-**I3** and triethylamine in *o*-dichlorobenzene under nitrogen. The reaction mixture was heated to 180 °C for 12 h. After cooling to the room temperature, and the solvent was evaporated in vacuo and the product was purified by chromatography on silica gel to give product **BN-PhTh**, **BN-BTTh** and **BN-BTBTh**.

4,9-Diphenyl-4,6,7,9-tetrahydrothieno[3',2':3,4][1,2]azaborinino[1,6,5-*de*]thieno[3',2':3,4] [1,2] azaborinino [5,6,1-*ij*]quinoxaline (BN-PhTh). I1 (0.50 g, 1.68 mmol), *o*-DCB (10 mL), dichlorophenylborane (0.80 g, 5.04 mmol) and triethylamine (0.7 mL, 5.04 mmol) were used, and CH_2Cl_2/*n*-hexane (v/v, 1:5) was used as the eluent to give product **BN-PhTh** as white powder (0.65 g, 82%). m.p., 206.4–207.8 °C. ^{1}H NMR (400 MHz, $CDCl_3$): δ 7.96 (s, 2H), 7.65-7.60 (m, 4H), 7.49-7.44 (m, 5H), 7.43-7.36 (m, 5H), 4.35 (s, 4H).^{13}C NMR (100 MHz, $CDCl_3$): δ 151.5, 133.1, 132.6, 129.0, 128.2, 128.1, 124.6, 121.5, 119.5, 47.2. HRMS (ESI-TOF) m/z: $[M + H]^+$ Calcd for $C_{28}H_{21}B_2N_2S_2$ 471.1332; Found 471.1342.

4,9-Diphenyl-4,6,7,9-tetrahydro-[1,2,5]thiadiazolo[3,4*g*]thieno[3',2':3,4][1,2]azaborinino[1,6,5-*de*]thieno[3',2':3,4][1,2]azaborinino[5,6,1-*ij*]quinoxaline (BN-BTTh). I2 (0.50 g, 1.40 mmol), *o*-DCB (10 mL), dichlorophenylborane (0.66 g, 4.20 mmol) and triethylamine (0.60 mL, 4.20 mmol) were used, and CH_2Cl_2/*n*-hexane (v/v, 1:5) was used as the eluent to give product **BN-BTTh** as orange powder (0.48 g, 65%). m.p. > 300 °C. ^{1}H NMR (400 MHz, $CDCl_3$): δ 7.66 (m, 6H), 7.53-7.43 (m, 8H), 4.46 (s, 4H). ^{13}C NMR (100 MHz, $CDCl_3$): δ 149.1, 148.2, 133.1, 132.7, 131.4, 129.0, 128.5, 128.2, 112.2, 47.6. HRMS (ESI-TOF) m/z: $[M + H]^+$ Calcd for $C_{28}H_{19}B_2N_4S_3$ 529.0958; Found 529.0968.

5,10-Diphenyl-5,7,8,10-tetrahydrobenzo[4',5']thieno[3',2':3,4][1,2]azaborinino[1,6,5-*de*] benzo[4',5']thieno[3',2':3,4][1,2]azaborinino[5,6,1-*ij*][1,2,5]thiadiazolo[3,4-*g*]quinoxaline (BN-BTBTh). I3 (0.50 g, 1.10 mmol), *o*-DCB (10 mL), dichlorophenylborane (0.69 g, 4.40 mmol) and triethylamine (0.65 mL, 4.40 mmol) were used, and CH_2Cl_2/*n*-hexane (v/v, 1:5) was used as the eluent to give product **BN-BTBTh** as yellow powder (0.43 g, 62%). Solid-state ^{13}C NMR (300 MHz): δ 149.5, 142.9, 141.1, 133.1, 129.9, 123.3, 118.0, 111.4, 46.7. HRMS (ESI-TOF) m/z: $[M + H]^+$ Calcd for $C_{36}H_{23}B_2N_4S_3$ 629.1271; Found: 629.1283.

Table S1. Crystal Data of **BN-PhTh** (CCDC: 1817703).

Experical formula	$C_{28}H_{20}B_2N_2S_2$
Space group	$Pna2_1$
Cell lengths	a/Å 11.9322 (5) b/Å 12.5611(4) c/Å 30.2148 (9)
Cell angles	α/° 90.00 β/° 90.00 γ/° 90.00
Cell volume	4528.64 /Å^3
Z, Z'	Z: 8 Z': 0
R-Factor (%)	4.68

Table S2. Crystal Data of **BN-BTTh** (CCDC:1817704).

Experical formula	$C_{28}H_{18}B_2N_4S_3$
Space group	P-1
Cell lengths	a/Å 7.816 (4) b/Å 12.150(5) c/Å 12.764 (6)
Cell angles	α/° 91.877 (9) β/° 92.37 (2) γ/° 91.526 (14)
Cell volume	1209.96 /Å^3
Z, Z'	Z: 2 Z': 0
R-Factor (%)	3.41

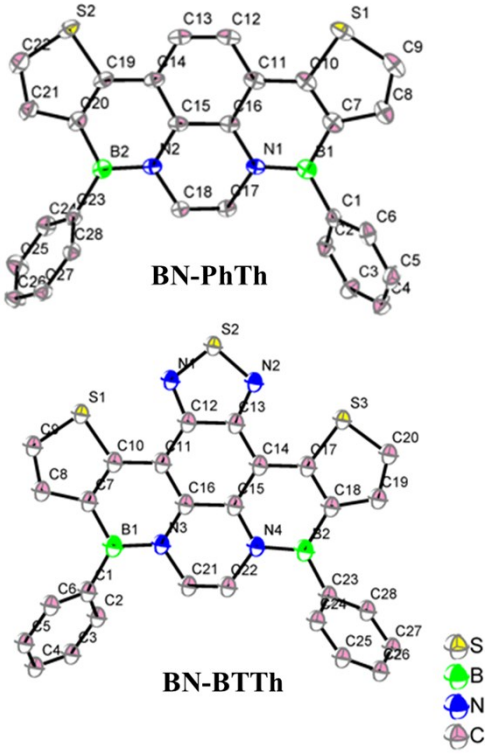

Fig. S1 ORTEP diagrams for the molecular structure of **BN-PhTh** and **BN-BTTh**. Thermal ellipsoids are drawn at the 50% probability level. Hydrogen atoms have been omitted for the sake of clarity.

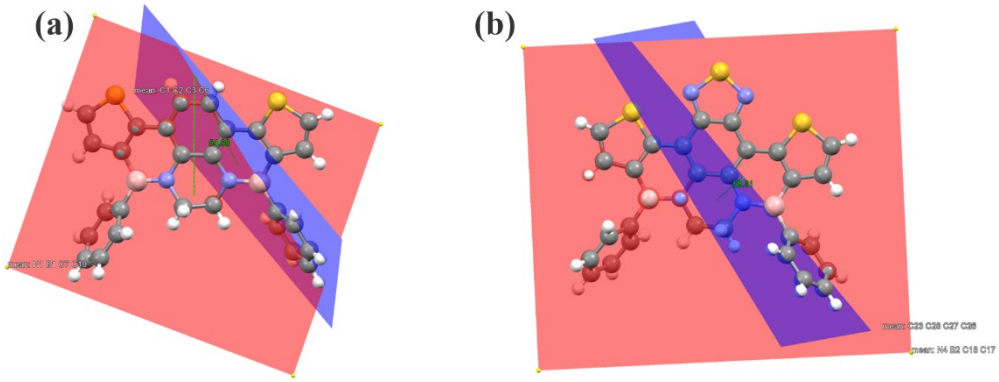

Fig. S2 Dihedral angles of (a) **BN-PhTh** and (b) **BN-BTTh**.

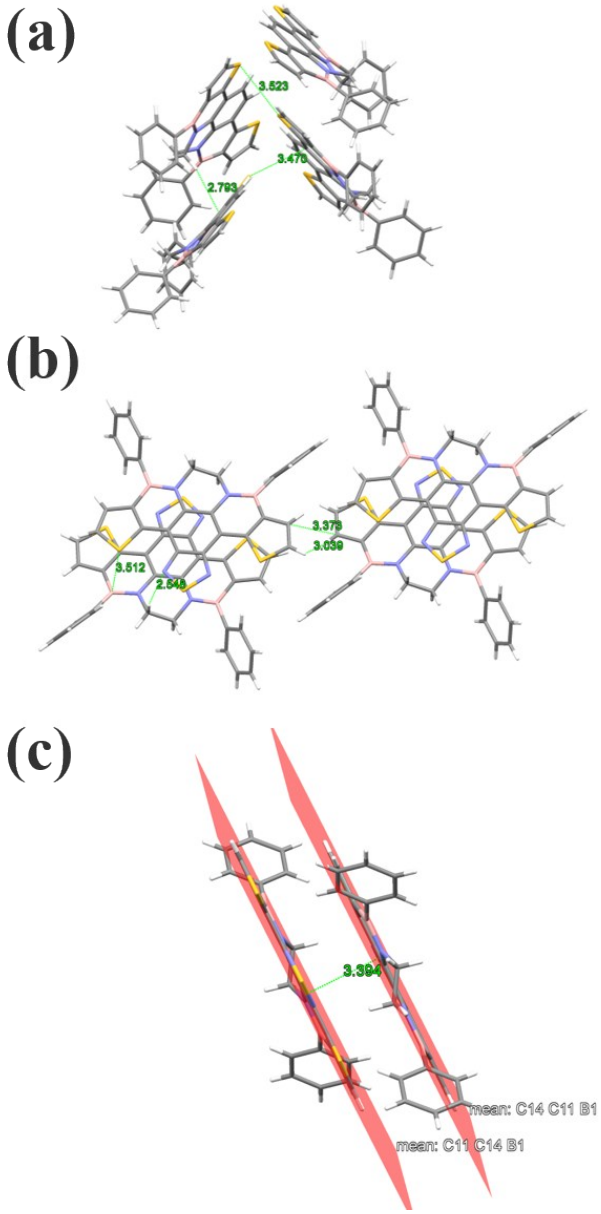

Fig. S3 Multiple intermolecular interactions of (a) **BN-PhTh** (b) **BN-BTTh** existed in the crystals, including S···S, S···π, N-H···π, B···S-C and C-H···π interactions. (c) The distance between the rigid planes of two molecules of **BN-BTTh**.

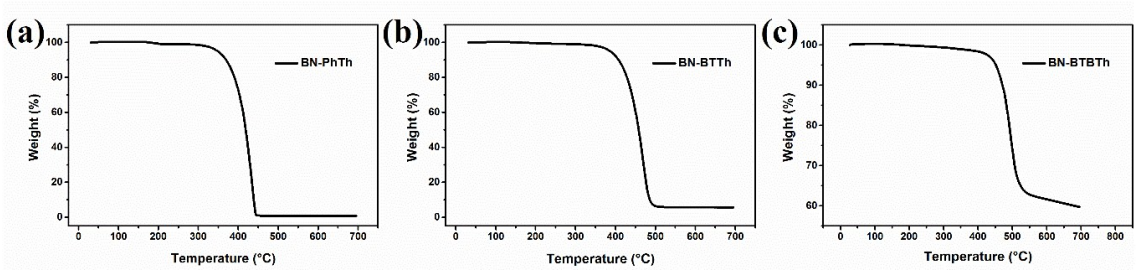

Fig. S4 Thermogravimetric analysis (TGA) of (a) **BN-PhTh** (5% weight loss: 348 °C), (b) **BN-BTTh** (5% weight loss: 392 °C) and (c) **BN-BTBTh** (5% weight loss: 440 °C).

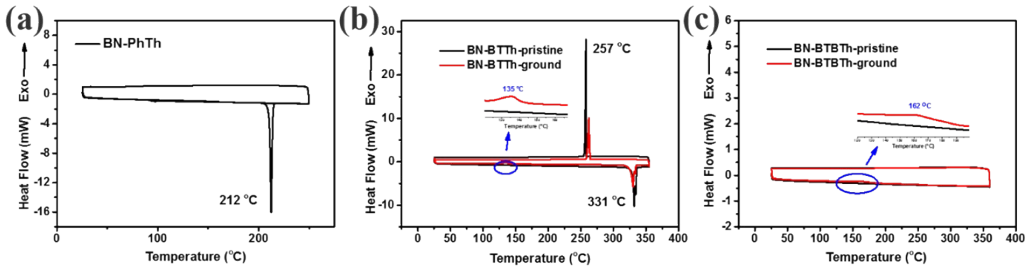

Fig. S5 DSC traces of (a) **BN-PhTh**, (b)**BN-BTTh** and (c) **BN-BTBTh**.

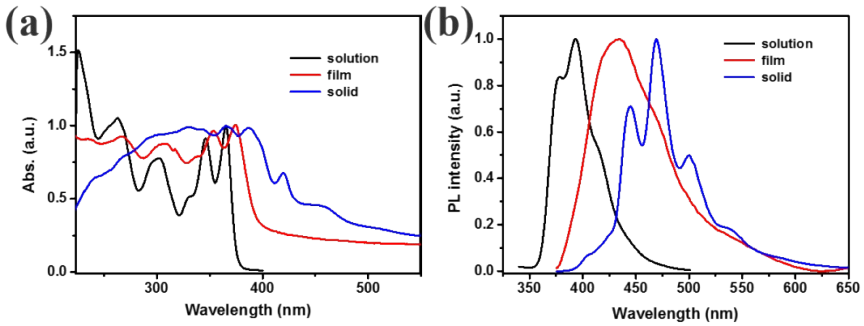

Fig. S6 (a) UV-vis absorption spectra, (b) fluorescence spectra of **BN-PhTh** in CH_2Cl_2, in film and in solid states.

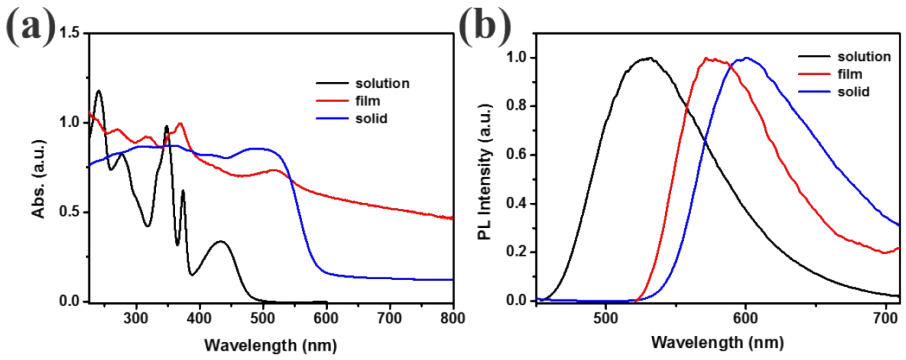

Fig. S7 (a) UV-vis absorption spectra, (b) fluorescence spectra of **BN-BTTh** in CH_2Cl_2, in film and in solid states.

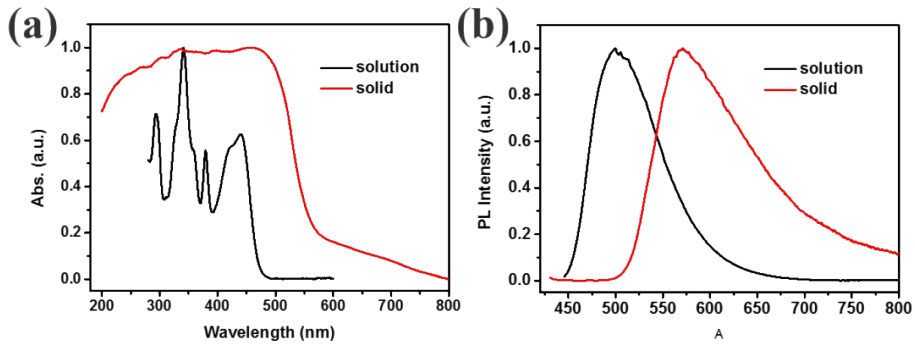

Fig. S8 (a) UV-vis absorption spectra, (b) fluorescence spectra of **BN-BTBTh** in CH_2Cl_2 and in solid states.

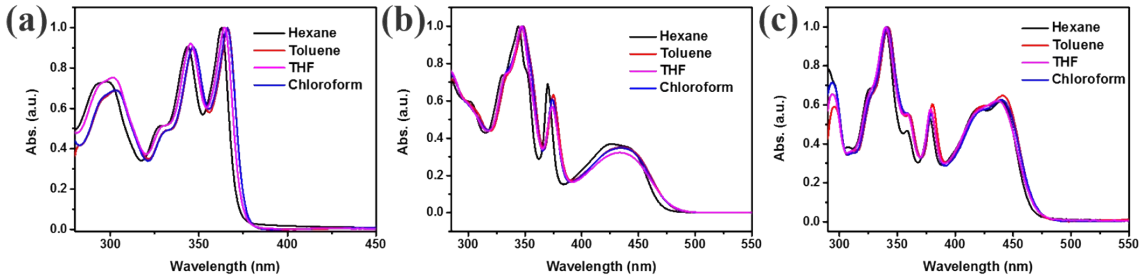

Fig. S9 UV-vis absorption spectra of (a) **BN-PhTh**, (b) **BN-BTTh** and (c) **BN-BTBTh** in different solvents.

Table S3. The Fluorescence Quantum Yields (Φ_F) of BN-PhTh, BN-BTTh and BN-BTBTh in Different Solvents

	Fluorescence Quantum Yields (Φ_F)[a]		
	BN-PhTh	**BN-BTTh**	**BN-BTBTh**
Hexane	36%	45%	42%
Toluene	31%	35%	37%
THF	27%	30%	26%
Chloroform	25%	28%	26%

[a] Measured using 9,10-diphenylanthracene in cyclohexane as standard (0.90)

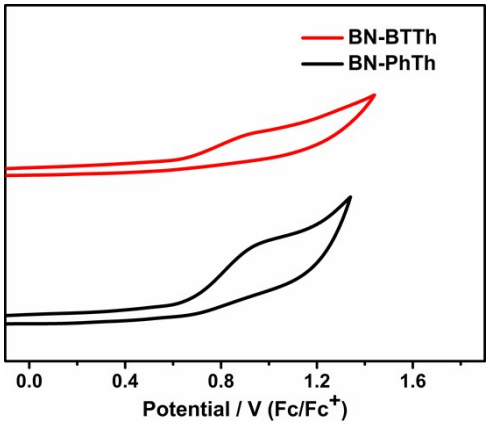

Fig. S10 CV curves of **BN-PhTh** and **BN-BTTh** in CH_2Cl_2 (1 mM) with 0.1 M *n*-Bu_4NPF_6 as supporting electrolyte.

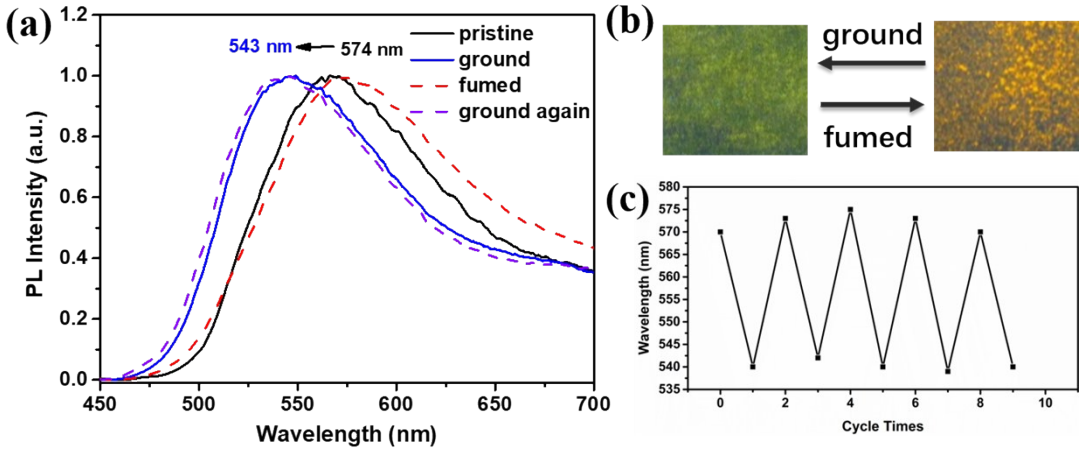

Fig. S11 (a) Normalized FL spectra of **BN-BTBTh** in different solid states excited at 435 nm. (b) The photographs of **BN-BTBTh** in different solid states under UV illumination at 365 nm.

(c) Switching the maximum solid-state emission wavelength of **BN-BTBTh** by repeated grinding-fuming processes.

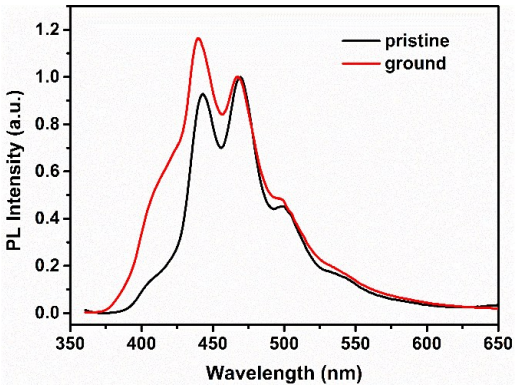

Fig. S12 Normalized FL spectra of **BN-PhTh** in different solid states excited at 345 nm.

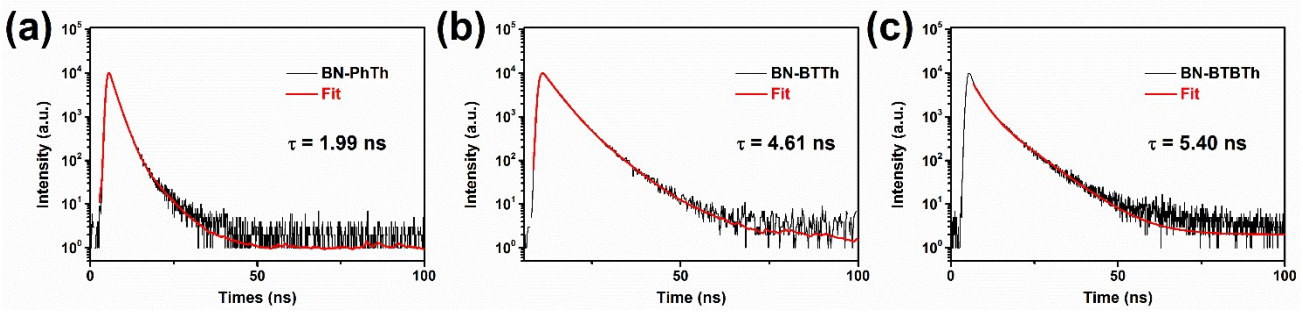

Fig. S13 Fluorescence decay curve (black line) of (a) **BN-PhTh** (b) **BN-BTTh** and (c) **BN-BTBTh** in pristine solid state. Red line: fitting of the fluorescence decay curve.

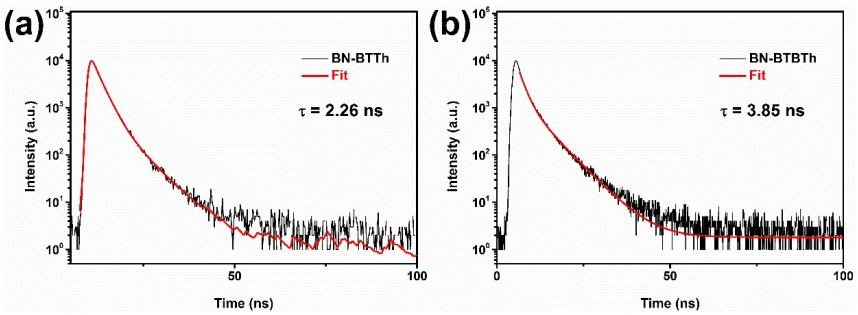

Fig. S14 Fluorescence decay curve (black line) of (a) **BN-BTTh** and (b) **BN-BTBTh** in ground solid state. Red line: fitting of the fluorescence decay curve.

Table S4. The Fluorescence Quantum Yields (Φ_F) of BN-PhTh, BN-BTTh and BN-BTBTh in Solid States

Compound	λ_{em} (nm)	$\Phi_{F\ pristine}$ (%)[a]	$\Phi_{F\ ground}$ (%)[a]
BN-PhTh	345	29.58	--
BN-BTTh	435	4.02	8.55
BN-BTBTh	435	35.20	40.25

[a] The fluorescence quantum yields were measured with an absolute fluorescence quantum yield spectrometer.

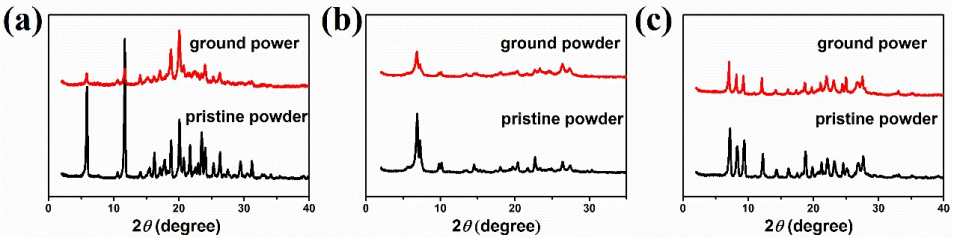

Fig. S15 PXRD patterns of (a) **BN-PhTh**, (b) **BN-BTTh** and (c) **BN-BTBTh** in different solid states.

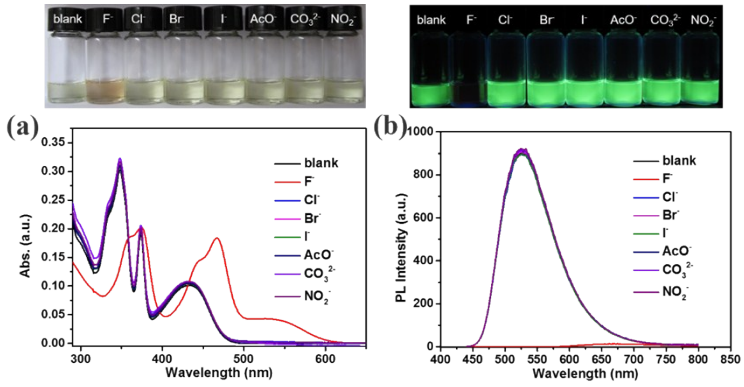

Fig. S16 BN-BTTh in THF (1 x 10^{-5} M) with addition of different anions (100 eq.): (a) Photographs under visible light and absorption spectra; (b) Photographs under UV light at 365 nm and fluorescence spectra (λ_{ex} = 435 nm).

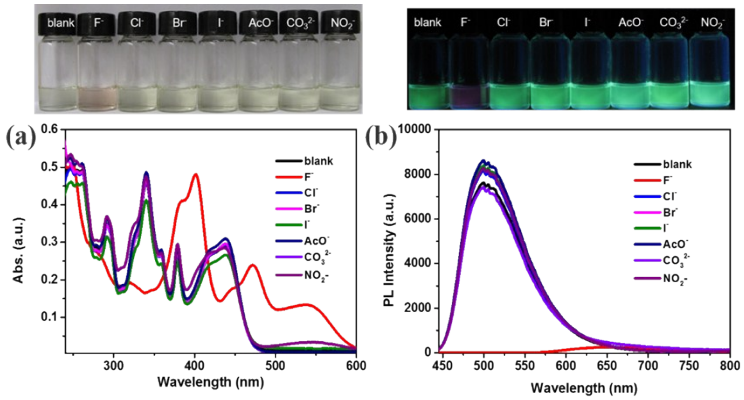

Fig. S17 BN-BTBTh in THF (1 x 10^{-5} M) with addition of different anions (100 eq.): (a) Photographs under visible light and absorption spectra; (b) Photographs under UV light at 365 nm and fluorescence spectra (λ_{ex} = 435 nm).

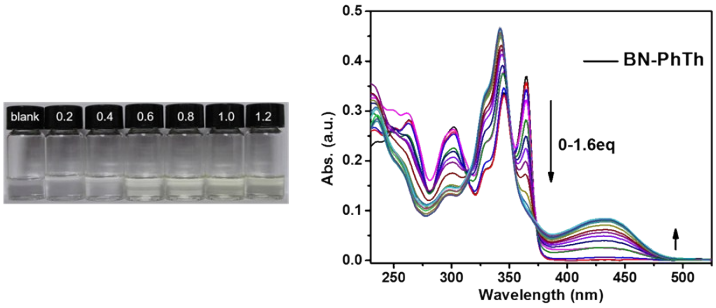

Fig. S18 BN-PhTh in THF (1 x 10^{-5} M) upon addition of TBAF photographs under visible light, and absorption spectra.

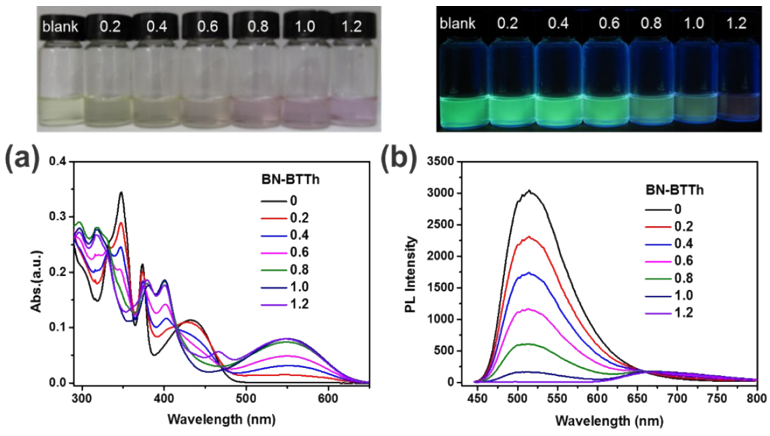

Fig. S19 (a) Photographs under visible light and absorption titration spectra of **BN-BTTh** (1 x 10^{-5} M in THF) upon addition of TBAF. (b) Photographs under UV light at 365 nm and fluorescence titration spectra of **BN-BTTh** (1 x 10^{-5} M in THF) upon addition of TBAF (λ_{ex} = 435 nm).

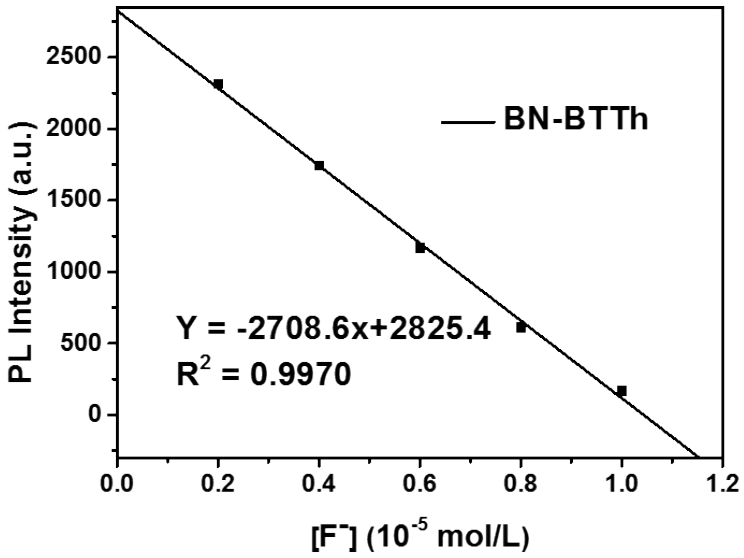

Fig. S20 The fluorescent intensity of **BN-BTTh** at 515 nm in different concentration of fluoride (λ_{ex} = 435 nm).

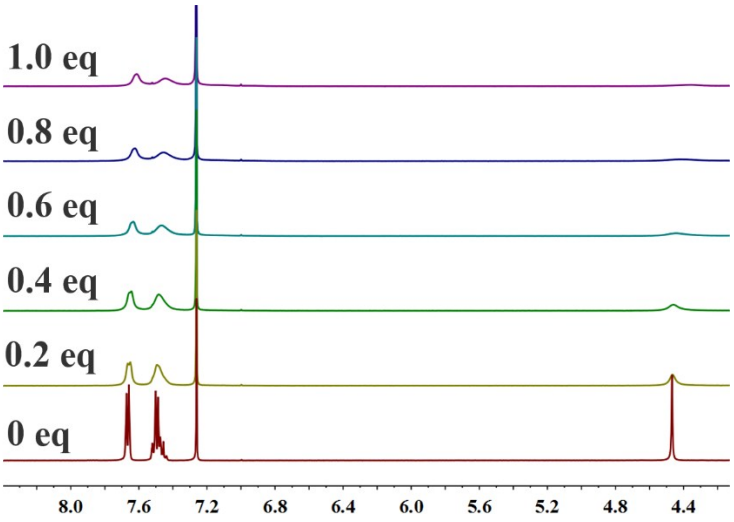

Fig. S21 ^{1}H NMR spectra of **BN-BTTh** (5 mM) in $CDCl_3$ in the presence of various equivalents of TBAF.

NMR and Mass Spectra:

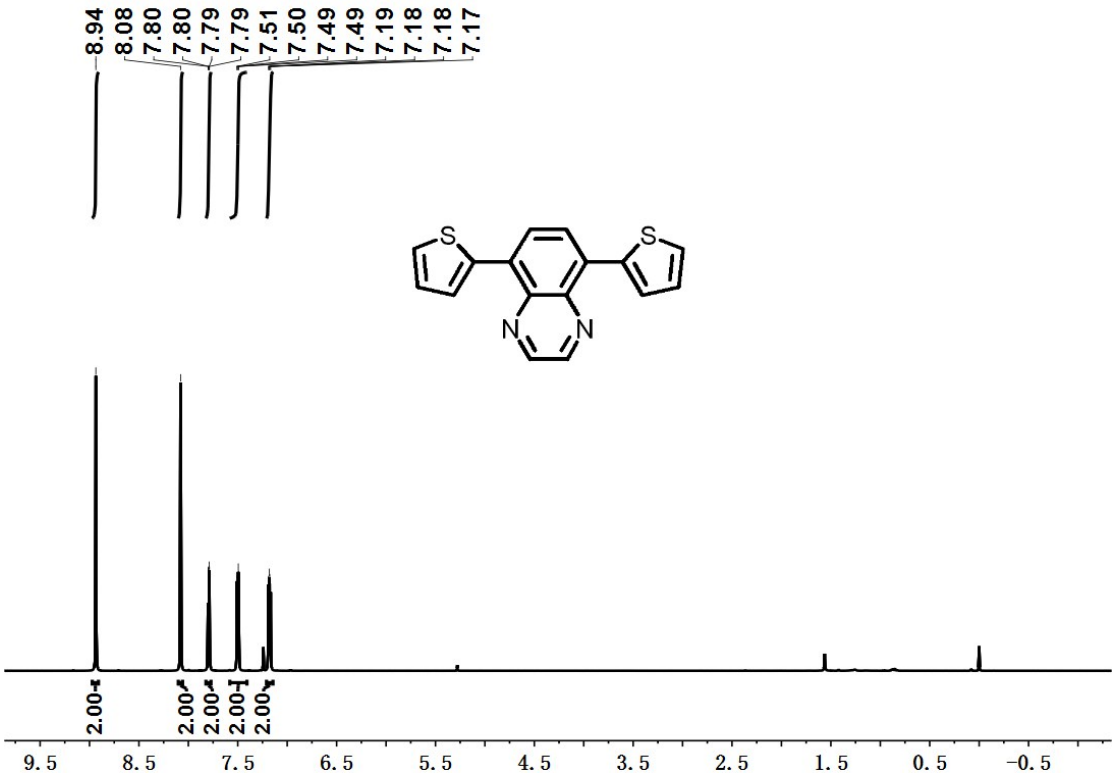

Fig. S22 ^{1}H NMR spectrum of compound **M1** in $CDCl_3$.

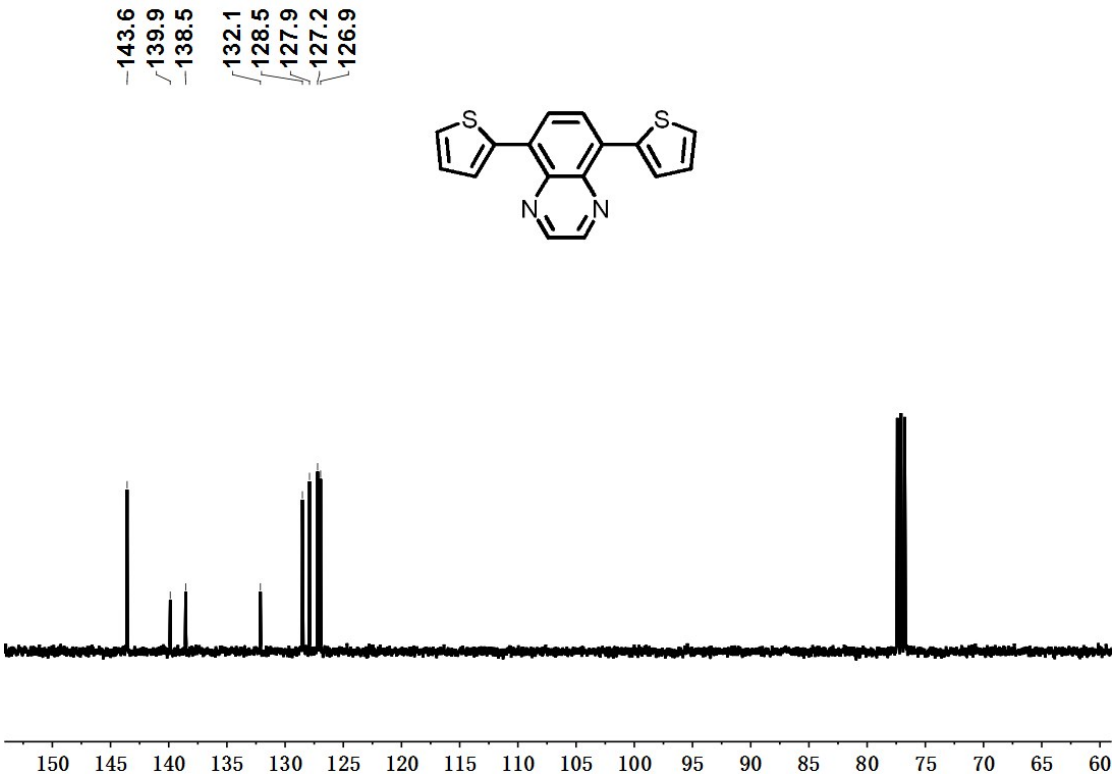

Fig. S23 ^{13}C NMR spectrum of compound **M1** in $CDCl_3$.

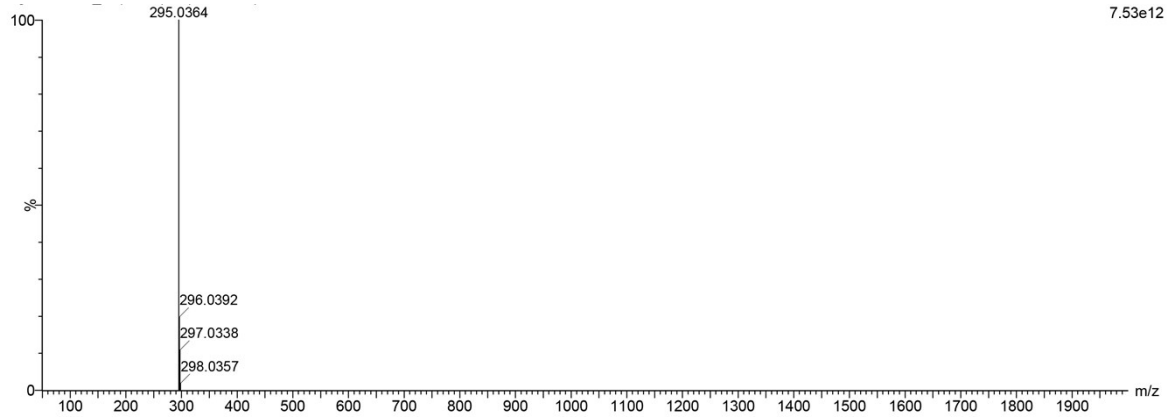

Fig. S24 ESI-TOF spectrum of compound **M1**.

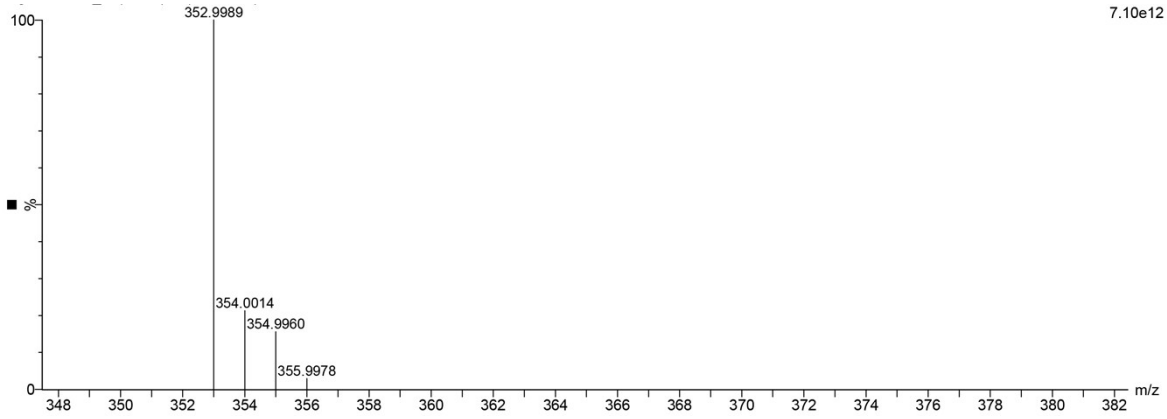

Fig. S25 ESI-TOF spectrum of compound **M2**.

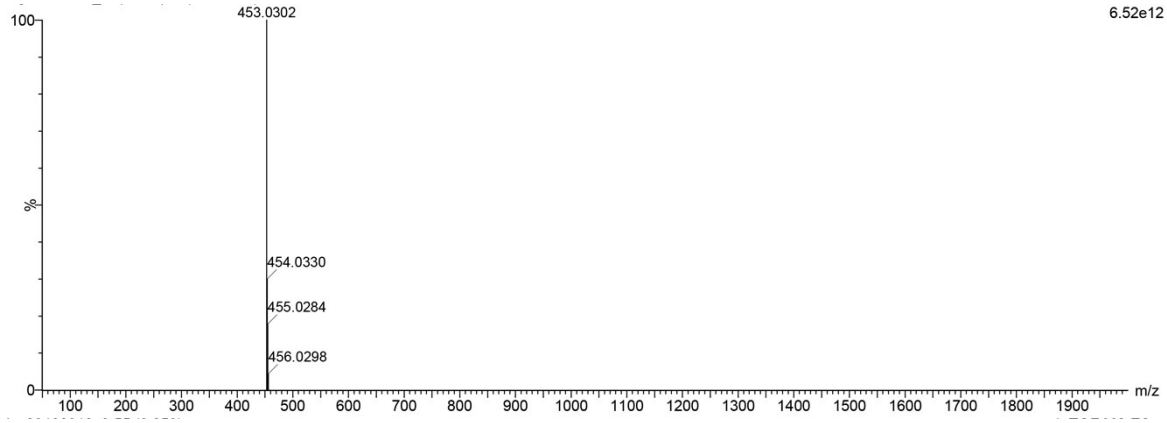

Fig. S26 ESI-TOF spectrum of compound **M3**.

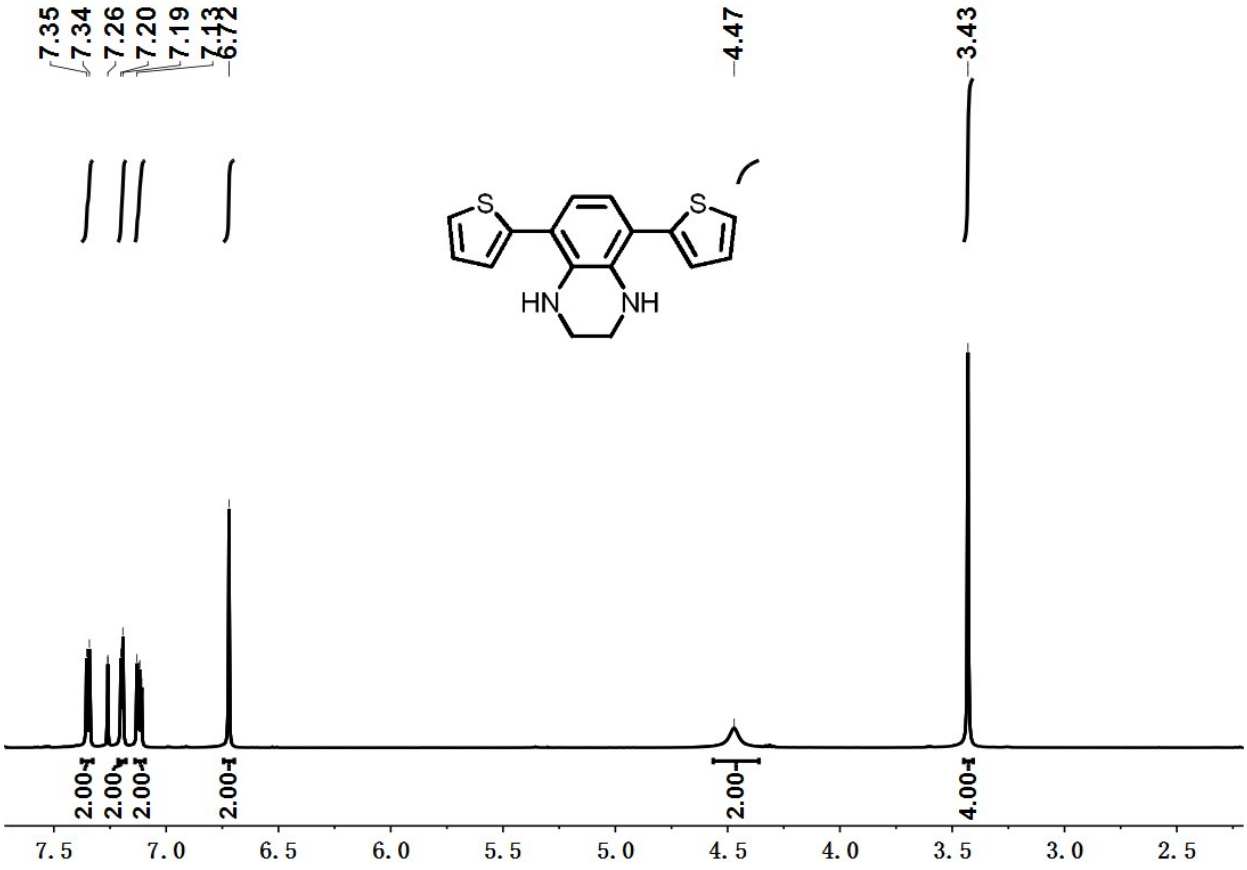

Fig. S27 ^{1}H NMR spectrum of compound **I1** in $CDCl_3$.

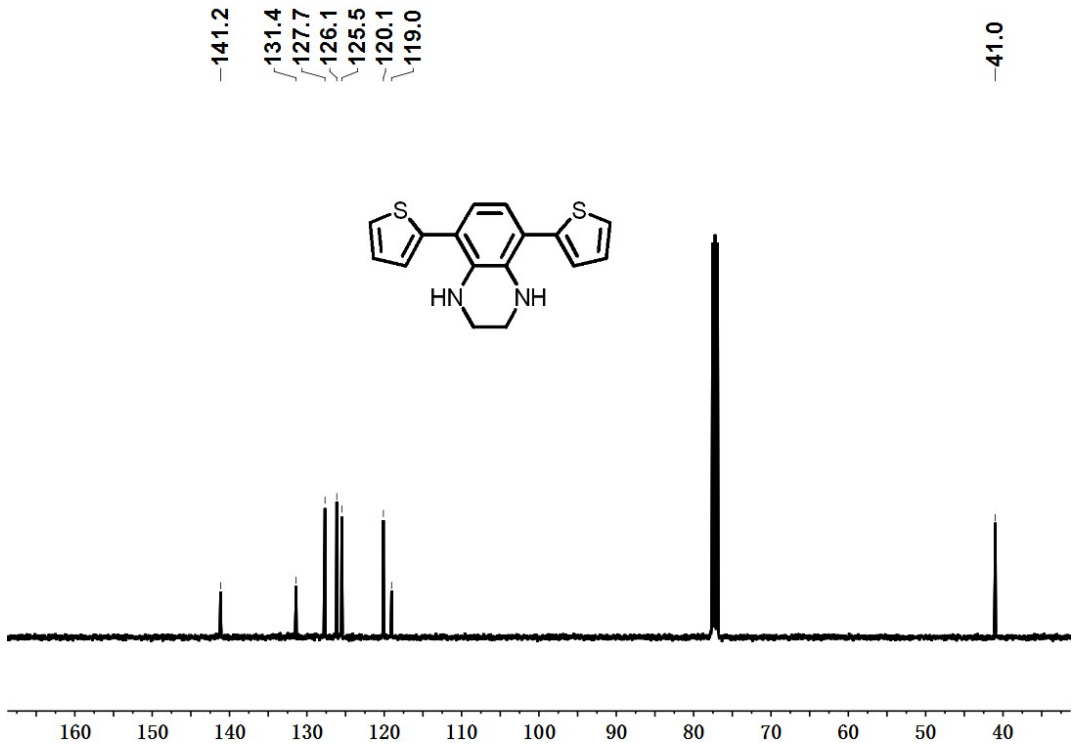

Fig. S28 ^{13}C NMR spectrum of compound **I1** in $CDCl_3$.

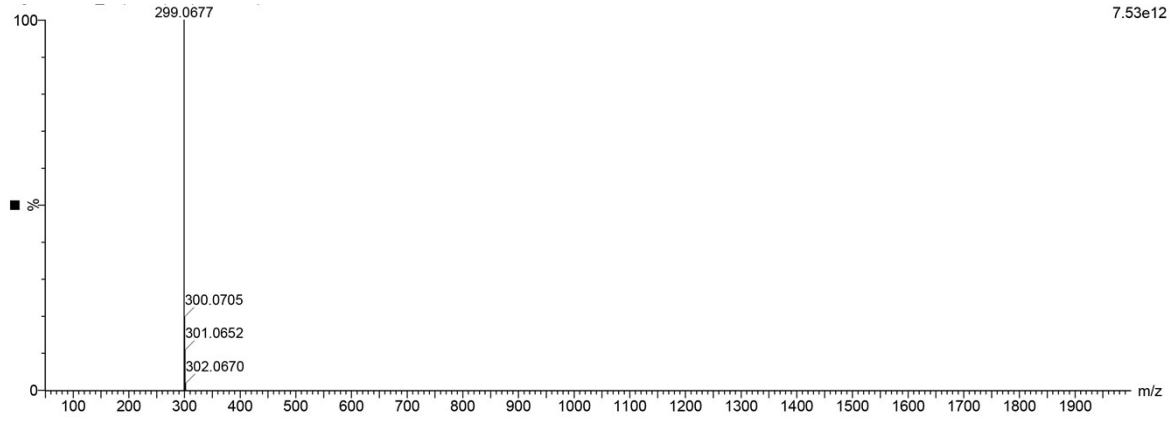

Fig. S29 ESI-TOF spectrum of compound **I1**.

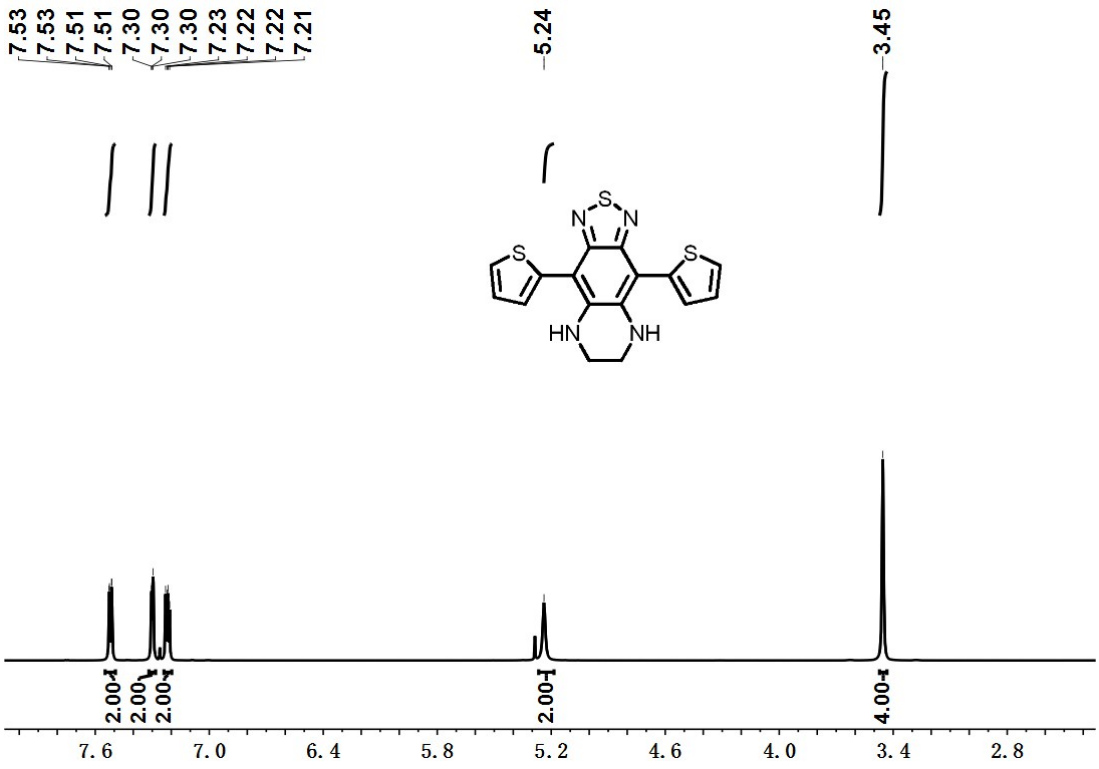

Fig. S30 ^{1}H NMR spectrum of compound **I2** in $CDCl_3$.

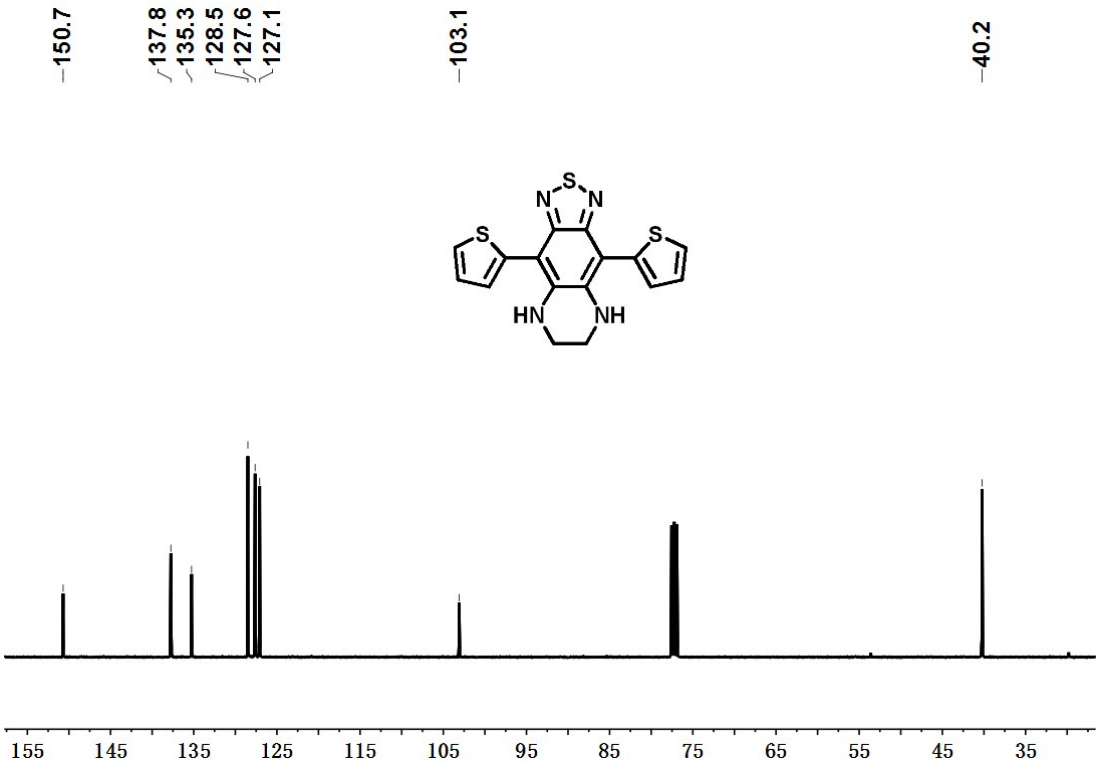

Fig. S31 ^{13}C NMR spectrum of compound **I2** in $CDCl_3$.

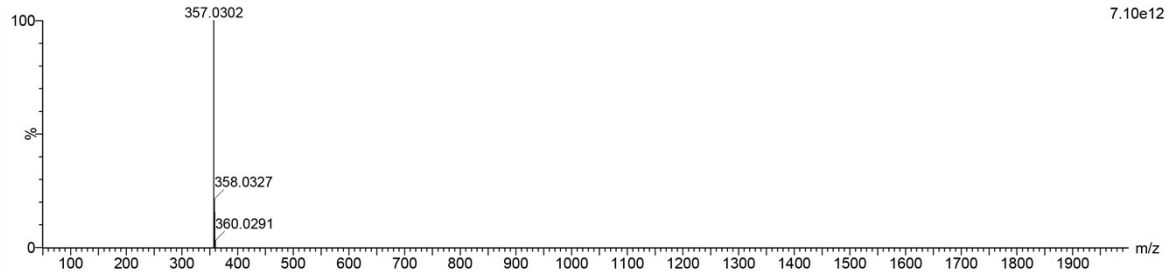

Fig. S32 ESI-TOF spectrum of compound **I2**.

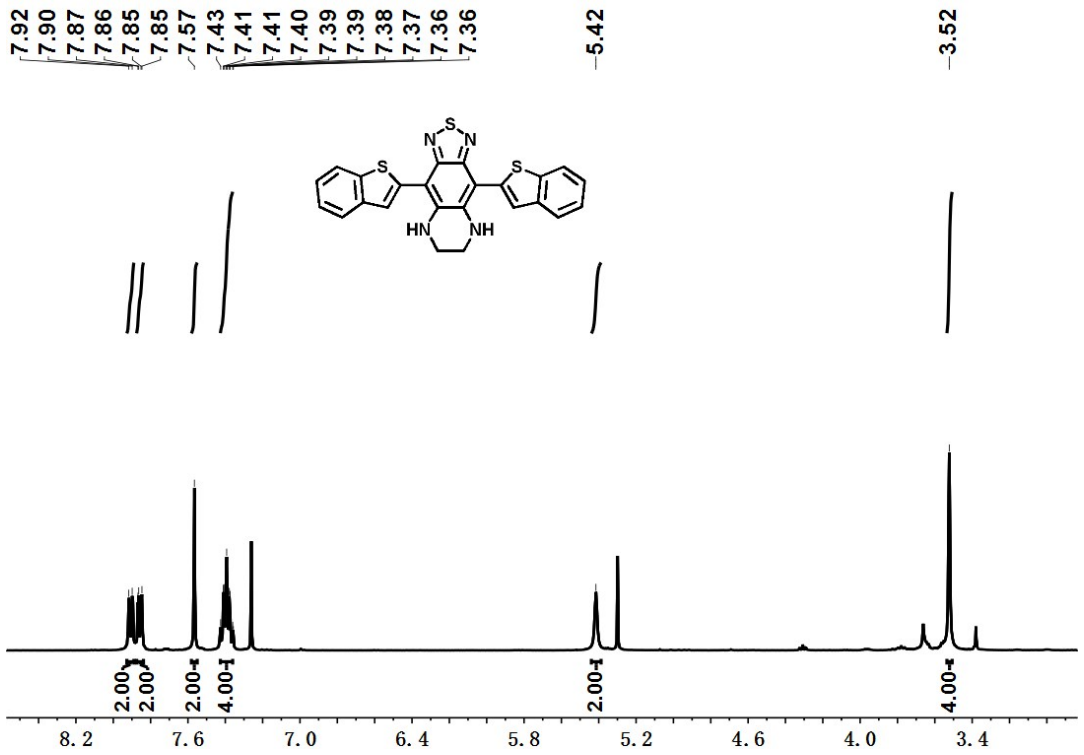

Fig. S33 ^{1}H NMR spectrum of compound **I3** in $CDCl_3$.

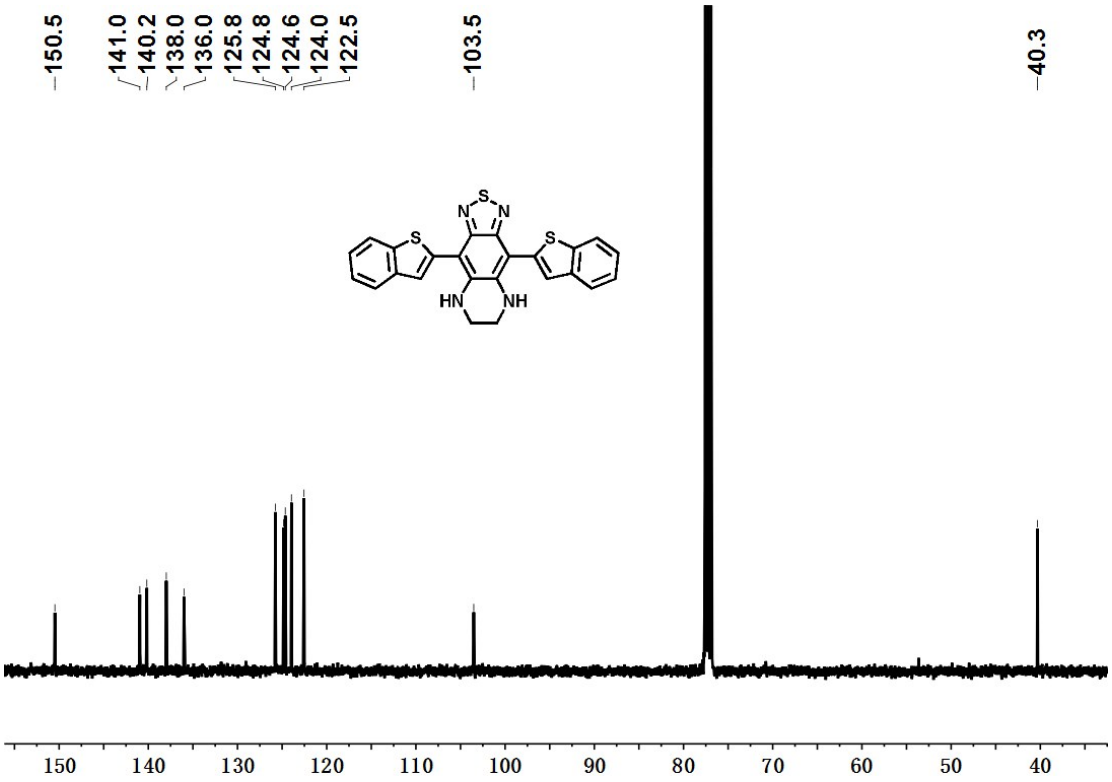

Fig. S34 ^{13}C NMR spectrum of compound **I3** in $CDCl_3$.

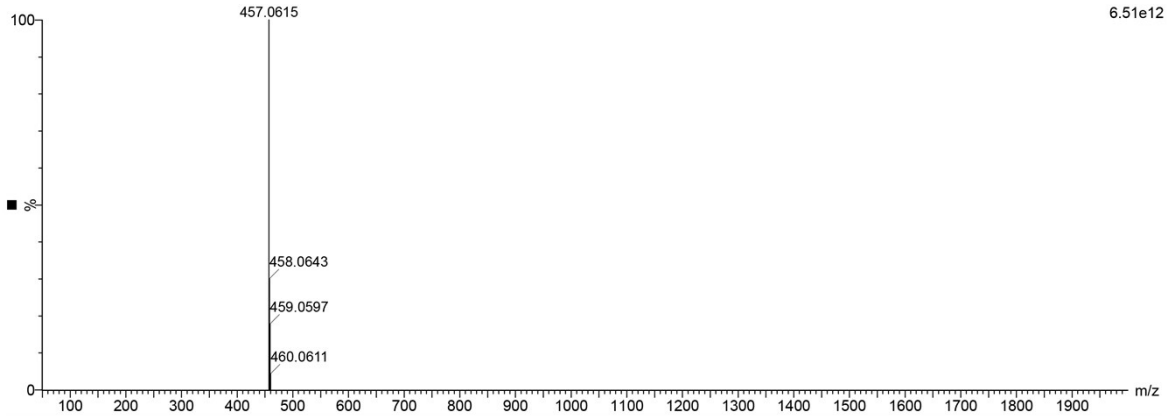

Fig. S35 ESI-TOF spectrum of compound **I3**.

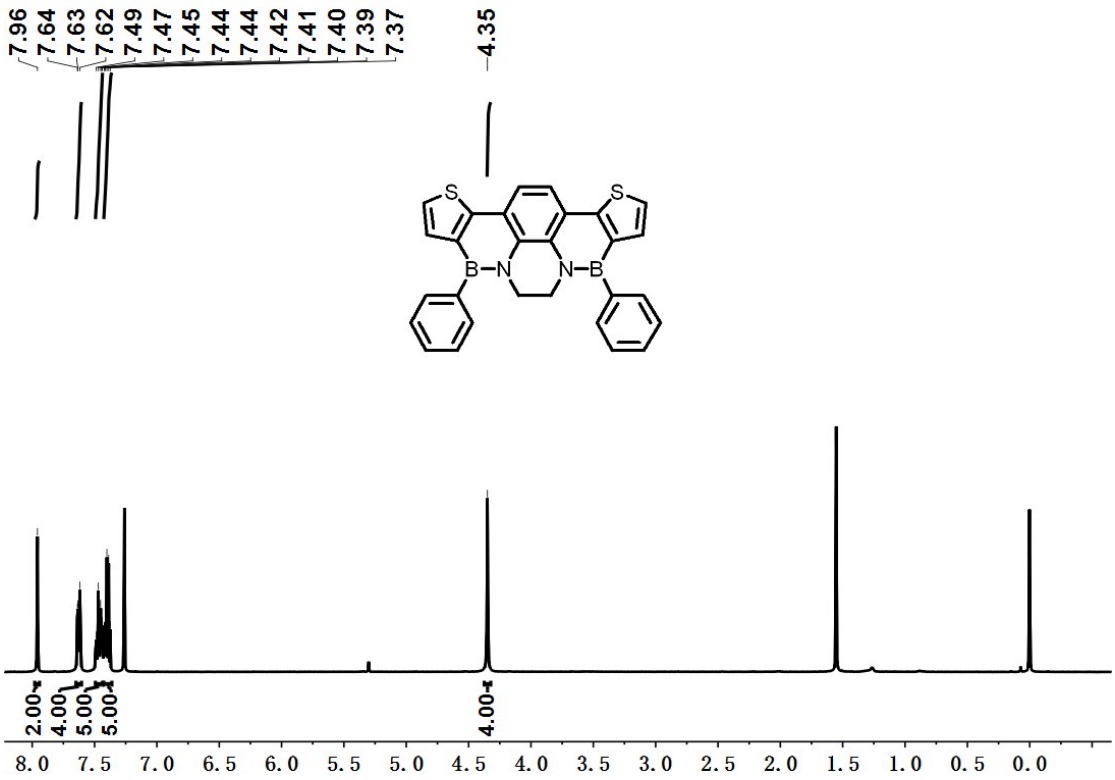

Fig. S36 ^{1}H NMR spectrum of **BN-PhTh** in $CDCl_3$.

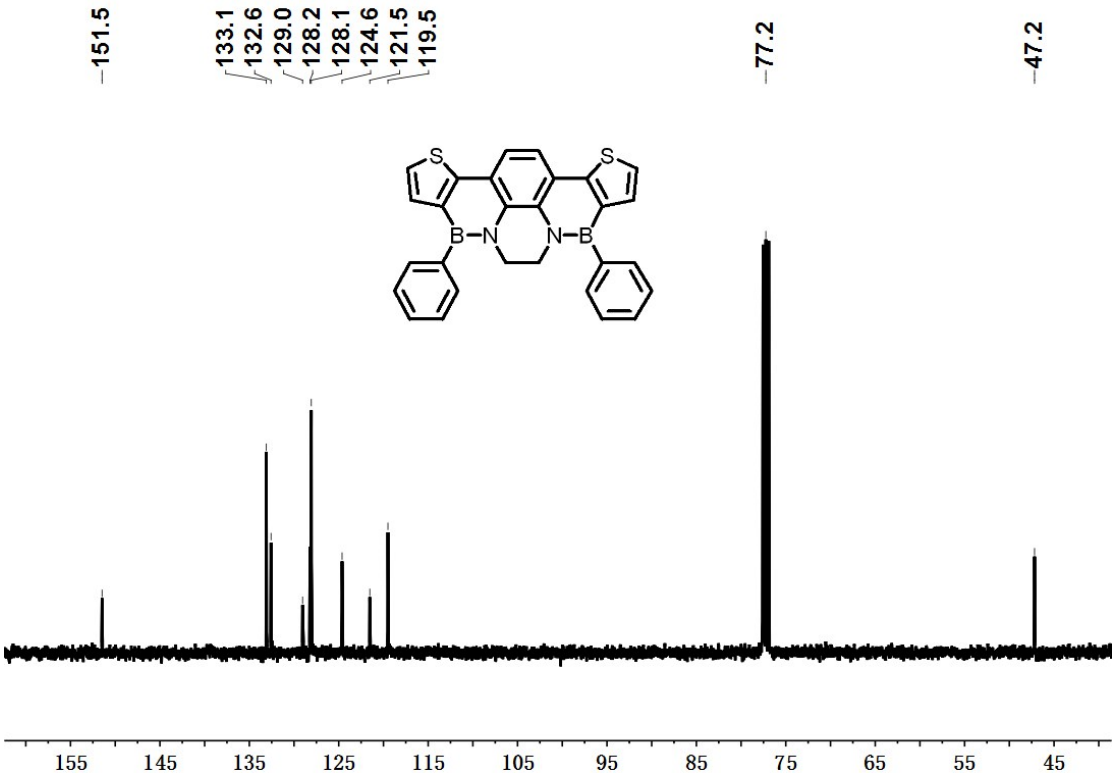

Fig. S37 ^{13}C NMR spectrum of **BN-PhTh** in $CDCl_3$.

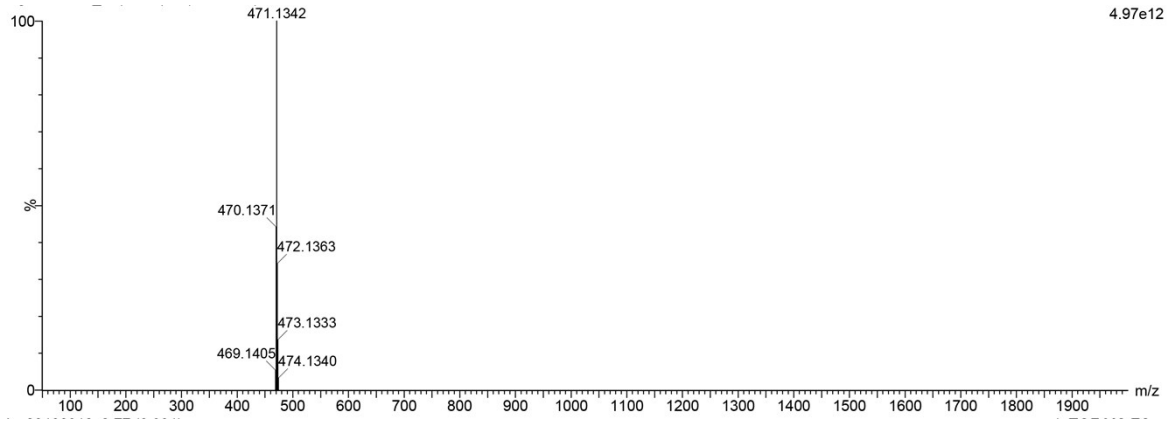

Fig. S38 ESI-TOF spectrum of **BN-PhTh**.

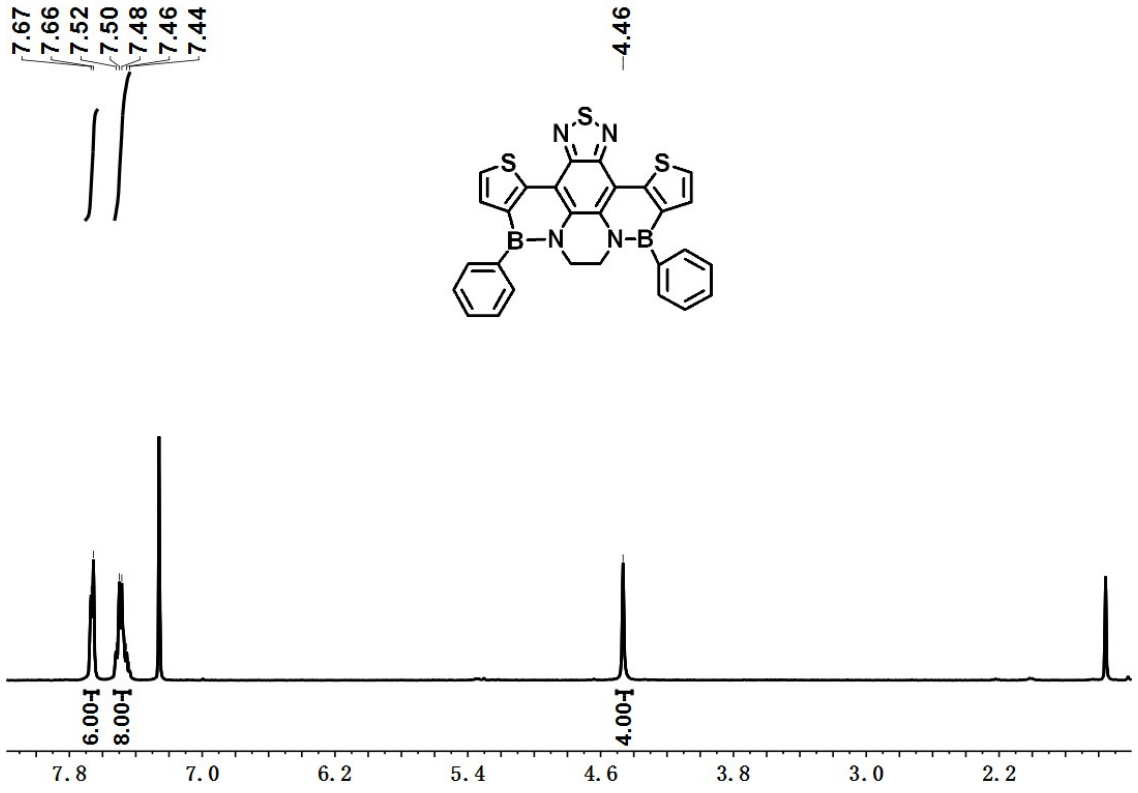

Fig. S39 ^{1}H NMR spectrum of **BN-BTTh** in $CDCl_3$.

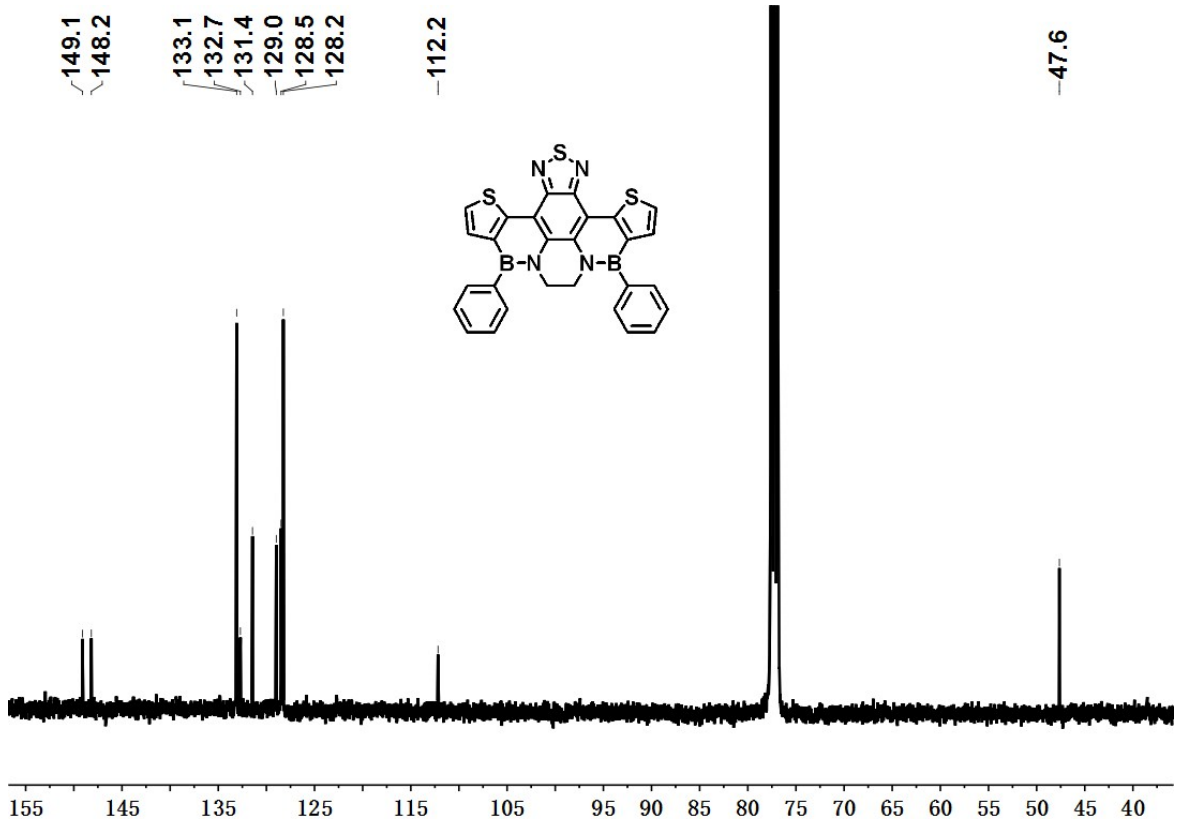

Fig. S40 ^{13}C NMR spectrum of **BN-BTTh** in $CDCl_3$.

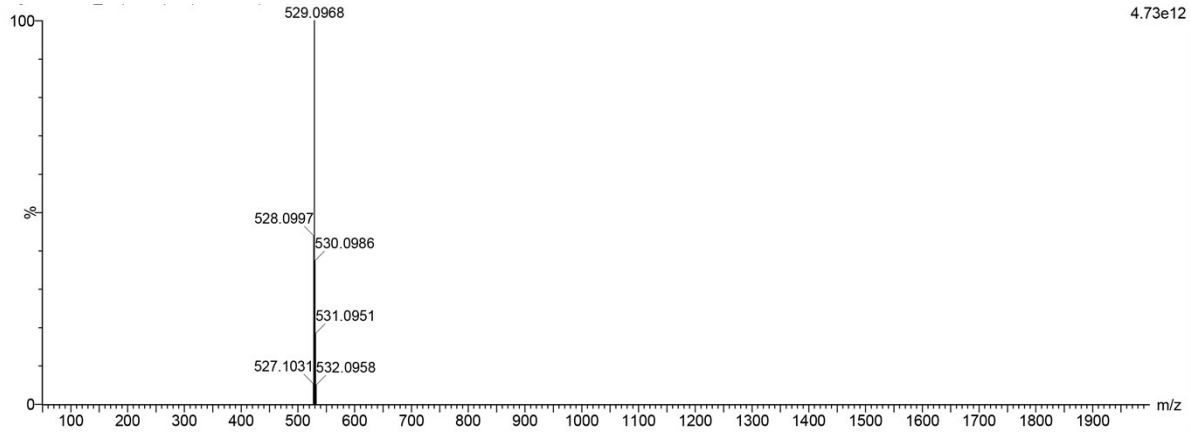

Fig. S41 ESI-TOF spectrum of **BN-BTTh**.

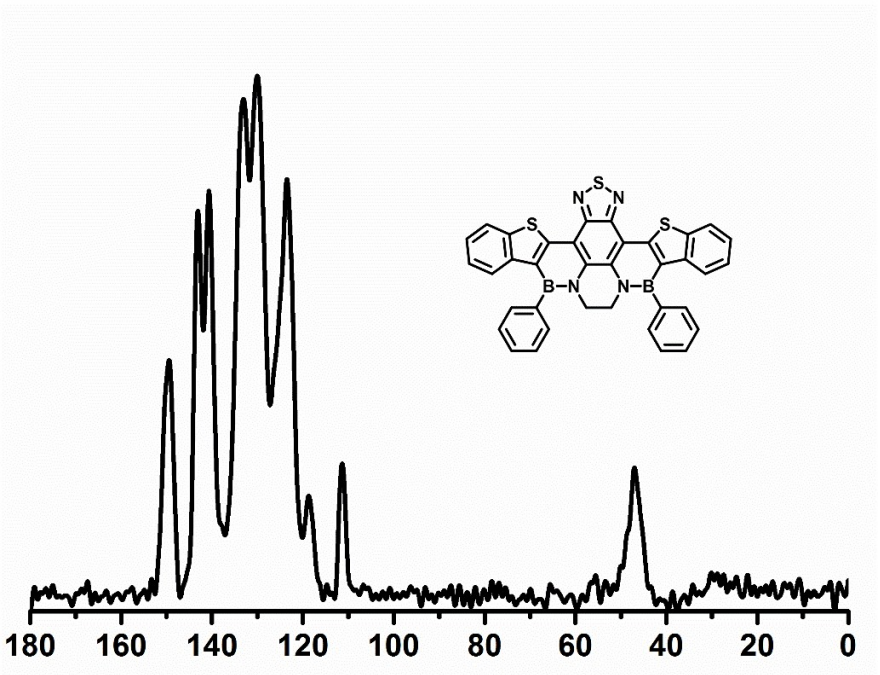

Fig. S42 ^{13}C NMR spectrum of **BN-BTBTh** in solid state.

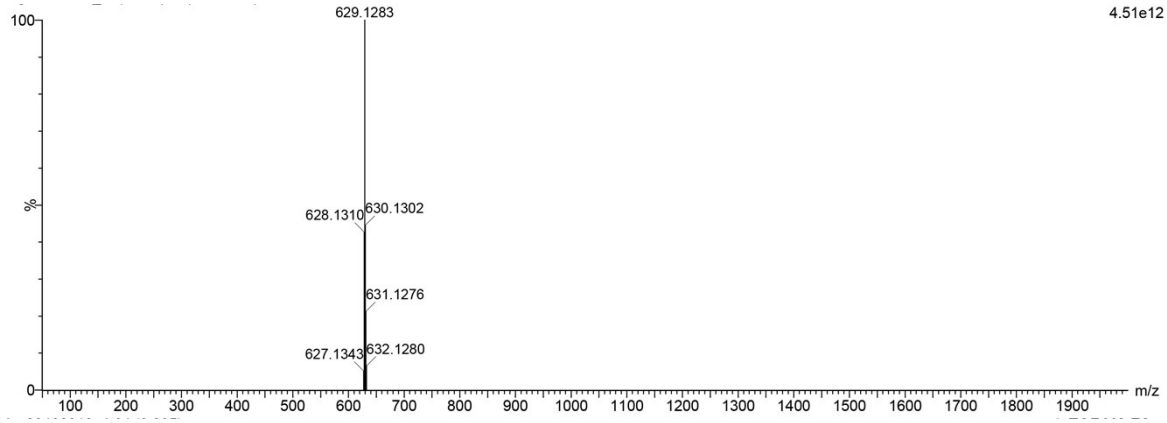

Fig. S43 ESI-TOF spectrum of **BN-BTBTh**.

Computational data for compounds BN-PhTh, **BN-BTTh**, **BT-BTBTh**:

Compound BN-PhTh

E = -2034.7717548 hartree

Center Number	Atomic Number	Atomic Type	Coordinates (Angstroms)		
			X	Y	Z
1	6	0	-1.413246	-2.106488	0.050568

2	6	0	0.718325	-0.869789	0.004177
3	6	0	-0.718328	-0.869788	-0.004205
4	6	0	-1.413249	-2.106486	0.050560
5	6	0	-0.683362	-3.318209	0.037827
6	6	0	0.683358	-3.318211	-0.037814
7	6	0	-2.848683	-2.090294	0.108114
8	6	0	2.848680	-2.090296	-0.108120
9	6	0	-3.611953	-0.927100	0.113612
10	6	0	-5.017136	-1.211203	0.207101
11	6	0	-5.298879	-2.542471	0.261641
12	16	0	-3.856665	-3.523165	0.206973
13	16	0	3.856662	-3.523170	-0.206938
14	6	0	5.298876	-2.542477	-0.261626
15	6	0	5.017133	-1.211208	-0.207120
16	6	0	3.611950	-0.927102	-0.113646
17	7	0	1.444116	0.330425	0.081665
18	7	0	-1.444119	0.330426	-0.081706
19	5	0	2.878164	0.408391	0.000025
20	6	0	3.648082	1.785992	0.042362
21	6	0	4.585504	2.051501	1.058657
22	6	0	5.312480	3.243162	1.089847
23	6	0	5.131993	4.199005	0.088799
24	6	0	4.219302	3.954989	-0.939305
25	6	0	3.488004	2.766384	-0.956346
26	5	0	-2.878168	0.408390	-0.000092
27	6	0	-3.648082	1.785994	-0.042388
28	6	0	-3.487943	2.766386	0.956310
29	6	0	-4.219237	3.954995	0.939308
30	6	0	-5.131984	4.199014	-0.088746
31	6	0	-5.312529	3.243172	-1.089784
32	6	0	-4.585556	2.051507	-1.058633
33	6	0	0.636443	1.512666	0.408838
34	6	0	-0.636446	1.512672	-0.408864
35	1	0	-1.222467	-4.260155	0.071601
36	1	0	1.222462	-4.260158	-0.071567
37	1	0	-5.779883	-0.440575	0.231720
38	1	0	-6.265632	-3.023414	0.334057
39	1	0	6.265629	-3.023422	-0.334026
40	1	0	5.779881	-0.440581	-0.231756
41	1	0	4.747547	1.313366	1.841421
42	1	0	6.022459	3.423505	1.893322
43	1	0	5.700737	5.125144	0.107004
44	1	0	4.078647	4.689190	-1.728809
45	1	0	2.786252	2.592520	-1.770493
46	1	0	-2.786145	2.592522	1.770417
47	1	0	-4.078535	4.689197	1.728803
48	1	0	-5.700723	5.125156	-0.106922
49	1	0	-6.022550	3.423517	-1.893221
50	1	0	-4.747645	1.313372	-1.841387

51	1	0	0.384726	1.498792	1.478456
52	1	0	1.223022	2.408403	0.212526
53	1	0	-1.223024	2.408406	-0.212536
54	1	0	-0.384732	1.498814	-1.478483

Compound BN-BTTh

E = -2541.246882 hartree

Center Number	Atomic Number	Atomic Type	Coordinates (Angstroms)		
			X	Y	Z
1	6	0	-1.449362	-1.593200	0.095239
2	6	0	0.728952	-0.384538	-0.024802
3	6	0	-0.744062	-0.384437	-0.030052
4	6	0	-1.472876	-1.581934	0.097232
5	6	0	-0.732130	-2.811911	0.098774
6	6	0	0.700035	-2.817782	-0.046179
7	6	0	-2.900475	-1.550083	0.181117
8	6	0	2.877300	-1.579807	-0.169529
9	7	0	1.228674	-4.037999	-0.079602
10	7	0	-1.267552	-4.026778	0.179762
11	16	0	-0.022031	-5.107047	0.070943
12	6	0	-3.633083	-0.359265	0.144033
13	6	0	-5.041182	-0.593294	0.281371
14	6	0	-5.353459	-1.912974	0.409015
15	16	0	-3.948347	-2.945073	0.370825
16	16	0	3.912745	-2.992195	-0.290071
17	6	0	5.330594	-1.977584	-0.323714
18	6	0	5.031760	-0.651573	-0.238953
19	6	0	3.622888	-0.396949	-0.153209
20	7	0	1.433070	0.818770	0.064941
21	7	0	-1.438219	0.818256	-0.169191
22	6	0	0.626048	2.033003	0.257301
23	6	0	-0.619014	1.961309	-0.589975
24	5	0	-2.875007	0.941038	-0.063024
25	5	0	2.876045	0.915022	0.012380
26	6	0	3.625670	2.297857	0.140483
27	6	0	-3.603533	2.336290	-0.175646
28	6	0	4.462093	2.745810	-0.900521
29	6	0	5.177097	3.940754	-0.801171
30	6	0	5.087932	4.714592	0.357104
31	6	0	4.277391	4.286773	1.410336
32	6	0	3.555172	3.097964	1.297471
33	6	0	-3.397872	3.368918	0.760250
34	6	0	-4.093386	4.576411	0.682586
35	6	0	-5.015004	4.786590	-0.344988

36	6	0	-5.240511	3.778848	-1.284061
37	6	0	-4.549081	2.569330	-1.192476
38	1	0	-5.778496	0.201901	0.282316
39	1	0	-6.333693	-2.357862	0.525994
40	1	0	6.308364	-2.437017	-0.397022
41	1	0	5.779510	0.133669	-0.230006
42	1	0	0.347419	2.134354	1.315085
43	1	0	1.229756	2.897059	-0.016719
44	1	0	-1.206685	2.871885	-0.493522
45	1	0	-0.342705	1.843870	-1.646770
46	1	0	4.553077	2.149511	-1.805985
47	1	0	5.807038	4.265115	-1.625777
48	1	0	5.648589	5.642076	0.440213
49	1	0	4.208448	4.878221	2.319978
50	1	0	2.932603	2.781079	2.132157
51	1	0	-2.689300	3.222339	1.573991
52	1	0	-3.918296	5.351437	1.424687
53	1	0	-5.556029	5.727023	-0.410549
54	1	0	-5.958062	3.932728	-2.086219
55	1	0	-4.746189	1.790933	-1.926493

Compound BN-BTBTh

E = -2848.5471862 hartree

Center Number	Atomic Number	Atomic Type	Coordinates (Angstroms)		
			X	Y	Z
1	6	0	-1.465934	-1.439400	0.056775
2	6	0	0.736120	-0.238016	-0.021083
3	6	0	-0.736133	-0.238034	0.021456
4	6	0	-1.465930	-1.439422	-0.056456
5	6	0	-0.718396	-2.667671	-0.052431
6	6	0	0.718412	-2.667658	0.052827
7	6	0	-2.895959	-1.415353	-0.099488
8	6	0	2.895968	-1.415333	0.099583
9	7	0	1.249959	-3.885400	0.095300
10	7	0	-1.249927	-3.885420	-0.094868
11	16	0	0.000018	-4.961242	0.000305
12	6	0	-3.639133	-0.234129	-0.055634
13	6	0	-5.066210	-0.490488	-0.146400
14	6	0	-5.355807	-1.872230	-0.247819
15	16	0	-3.900753	-2.860984	-0.232197
16	16	0	3.900777	-2.860965	0.232178
17	6	0	5.355840	-1.872218	0.247463
18	6	0	5.066234	-0.490481	0.146023
19	6	0	3.639141	-0.234116	0.055528
20	7	0	1.431551	0.959652	-0.151767

21	6	0	0.612919	2.146650	-0.437959
22	6	0	-0.612964	2.146614	0.438282
23	7	0	-1.431586	0.959633	0.152032
24	6	0	6.664656	-2.352546	0.346878
25	6	0	7.708718	-1.433758	0.347344
26	6	0	7.446372	-0.056919	0.250638
27	6	0	6.144450	0.416556	0.150797
28	6	0	-6.144418	0.416557	-0.151440
29	6	0	-7.446324	-0.056914	-0.251511
30	6	0	-7.708661	-1.433757	-0.348192
31	6	0	-6.664606	-2.352552	-0.347468
32	5	0	-2.874692	1.067378	0.116297
33	5	0	2.874671	1.067399	-0.116196
34	6	0	3.551818	2.488052	-0.279316
35	6	0	-3.551859	2.488020	0.279431
36	6	0	3.998779	2.944136	-1.533573
37	6	0	4.613939	4.189173	-1.678872
38	6	0	4.800826	5.011933	-0.566567
39	6	0	4.369474	4.580686	0.689163
40	6	0	3.753645	3.334855	0.827349
41	6	0	-3.753293	3.335039	-0.827137
42	6	0	-4.369136	4.580860	-0.688914
43	6	0	-4.800892	5.011877	0.566756
44	6	0	-4.614386	4.188906	1.678969
45	6	0	-3.999206	2.943884	1.533634
46	1	0	1.213403	3.036409	-0.258330
47	1	0	0.316063	2.143549	-1.495542
48	1	0	-0.316091	2.143430	1.495860
49	1	0	-1.213460	3.036381	0.258729
50	1	0	6.861824	-3.418165	0.423241
51	1	0	8.733947	-1.785542	0.424277
52	1	0	8.273318	0.647944	0.254410
53	1	0	5.956694	1.481347	0.078026
54	1	0	-5.956670	1.481350	-0.078688
55	1	0	-8.273265	0.647954	-0.255487
56	1	0	-8.733877	-1.785538	-0.425307
57	1	0	-6.861768	-3.418174	-0.423807
58	1	0	3.870970	2.313367	-2.411044
59	1	0	4.949772	4.515412	-2.660072
60	1	0	5.281429	5.980528	-0.677012
61	1	0	4.514822	5.212410	1.561968
62	1	0	3.431180	3.013464	1.816094
63	1	0	-3.430505	3.013831	-1.815835
64	1	0	-4.514177	5.212755	-1.561645
65	1	0	-5.281504	5.980465	0.677228
66	1	0	-4.950527	4.514973	2.660120
67	1	0	-3.871691	2.312948	2.411028

References.

1 C. Kitamura, S. Tanaka and Y. Yamashita, *Chem. Mater.*, 1996, **8**, 570-578.

2 Y. Tsubata, T. Suzuki, Y. Yamashita, T. Mukai and T. Miyashi, *Heterocycles*, 1992, **33**, 337-348.

3 C. Istanbulluoglu, S. Goker, G. Hizalan, S. O. Hacioglu, Y. A. Udum, E. D. Yildiz, A. Cirpan and L. Toppare, *New J. Chem.*, 2015, **39**, 6623-6630.

4 L. Torun, B. K. Madras and P. C. Meltzer, *Biorg. Med. Chem.*, 2012, **20**, 2762-2772.